Templated growth of a complex nitride island dispersion through an internal nitridation reaction

M.P. Brady,[a] D.T. Hoelzer, E.A. Payzant, P.F. Tortorelli, J.A. Horton, I.M. Anderson, and L.R. Walker
Metals and Ceramics Division, Oak Ridge National Laboratory, Oak Ridge, Tennessee 37831-6115

S.K. Wrobel
Department of Materials Science and Engineering, University of Tennessee, Knoxville, Tennessee

(Received 14 June 2001; accepted 2 August 2001)

A new synthesis route, based on internal oxidation reactions in multiphase alloys, is proposed for the controlled production of near-surface, complex ceramic-ceramic or ceramic-metallic composite structures. Using this approach, a microdispersion of a complex nitride perovskite, Cr_3PtN, was formed in Cr_2N or Cr(Pt) by internal nitridation of a two-phase Cr(Pt) + Cr_3Pt precursor alloy. A framework for use of this phenomenon to synthesize island micro- (and potentially meso- or nano-) composite functional surface structures is presented.

Internal oxidation (nitridation, sulfidation, carburization, boronization, etc.) reactions[1–5] provide a straightforward and rapid method to synthesize ceramic dispersions (oxides, nitrides, sulfides, carbides, borides, etc.). A major limitation from a synthesis standpoint is that internal oxidation usually yields only simple, binary ceramic precipitates (e.g., A_XX_Z). Although simple ceramic phases exhibit many interesting properties (e.g., Ref. 6), complex ceramic phases (e.g., ternary $A_xB_yX_z$ and higher order structures) offer a far greater wealth of behaviors and opportunities.[7–11] Complex ceramic phases have been reported as a result of internal oxidation (e.g., Ref. 12). However, they are typically formed by subsequent solid-state reactions involving the initially precipitated simple binary ceramic compound(s) with each other or the matrix. The particle size tends to be large (order of microns) and the chemistry varied, often irregularly intermixed with the initially formed binary ceramic compounds that gave rise to them. To solve this limitation, we propose that by using a *multiphase* alloy precursor, internal oxidation can be used to controllably synthesize *complex* ceramic island structures.

From a phenomenological viewpoint there are two limiting cases for the oxidation of a multiphase alloy (Fig. 1): (i) The phases may react cooperatively yielding a single-phase reaction product or (ii) the phases may react independently yielding a composite reaction product (e.g., Refs. 13–17). The cooperative phenomenon [Fig. 1(a)] has been used as a basis to design heat-resistant alloys for use in oxidizing environments and is of long-standing technological importance. The independent reaction mode was first reported in the late 1950s (Ref. 18) but has been considered of little direct technological importance, with only a small number of studies in the intervening 40 years (reviewed in Ref. 17). The key characteristic of the independent reaction mode, recently termed "*in situ*" or "in-place" internal oxidation,[17,19] is that the reaction is dominated by inward oxidant transport, with negligible outward diffusion of the alloy components within the individual phases. Consequently, the reaction product replicates the size, morphology, spatial distribution, and chemistry of each phase in the underlying alloy structure [Fig. 1(b)]. Effectively, the initial alloy microstructure acts as a *template*. If the second phase is a multicomponent metallic (or intermetallic) compound, we propose that a complex ceramic phase with a similar metal component stoichiometry can potentially be formed.

To determine whether the direct, controlled formation of a complex ceramic phase dispersion from a precursor metal precipitate phase of similar metal component stoichiometry is possible, we examined the nitridation behavior of Cr-5Pt atomic percent (at.%). This alloy consists of a dilute Cr(Pt) matrix with a Cr_3Pt second-phase precipitate and was selected for study because Cr exhibits a high permeability for nitrogen, which favors internal modes of reaction, and a complex nitride phase with similar metal component stoichiometry to Cr_3Pt, the Cr_3PtN perovskite phase,[20] exists. The alloy was arc cast from high-purity Cr and Pt chips and nitrided for 48 h at 1100 °C (as-cast) or 24 h at 1000 °C (after a 1350 °C-8

[a]Address all correspondence to this author.
bradymp@ornl.gov

 © 2001 Materials Research Society

h/1050 °C-12 h solution/precipitation vacuum heat treatment) in high-purity nitrogen. The nitrided samples were characterized by x-ray diffraction (XRD) using Cu K_α radiation (1.5406 Å), scanning electron microscopy (SEM), electron probe microanalysis (EPMA) using pure element standards for Cr, Pt, and a BN standard for nitrogen, and transmission electron microscopy (TEM). All compositions are reported in at.%.

Cross-section SEM micrographs for heat treated Cr-5Pt after 24-h nitridation at 1000 °C are shown in Fig. 2. The microstructure consisted of three zones: a 3-μm surface Cr-nitride layer of composition 74Cr–26N, a second layer approximately 75 μm thick of nitrided Cr(Pt) matrix of composition 69Cr-1Pt-30N containing a dispersion of nitrided Cr_3Pt (white) of composition 65Cr-13Pt-22N, and a third zone an additional ≈100 μm deep containing nitrided Cr_3Pt (white) of composition 69Cr-16Pt-15N in a matrix of metallic Cr(Pt) of composition 99Cr-1Pt. The composition of the Cr_3Pt phase away from the reaction zone was approximately 86Cr-14Pt. [The compositions of the Cr_3Pt and nitrided Cr_3Pt regions should be considered semiquantitative due to the likelihood of beam overlap with the surrounding Cr rich regions as a result of the fine (generally micron-range size) alloy structure.] The nitrided microstructure suggests an initial, transient period of cooperative reaction to form an external Cr-nitride surface layer followed by a transition to extensive subscale in-place internal nitridation, which replicated the underlying alloy structure.

By SEM and EPMA analysis, most of the nitrided Cr_3Pt particles (white) appeared single phase [Fig. 2(b)]. Some of the nitrided Cr_3Pt particles showed a small "sliver" of a dark phase region in the center of the particle, suggesting the presence of a small fraction of a second phase. This may be due to incomplete nitridation or possibly an artifact of the fine scale of the nitrided Cr_3PtN precipitates in which underlying regions of the nitrided Cr-matrix phase may show through.

XRD analysis indicated that the outer Cr-rich nitride surface layer was Cr_2N. Additional analysis was performed on an as-cast, 48 h, 1100 °C nitrided coupon from which the surface Cr_2N layer was removed by grinding (Fig. 3). The diffraction pattern was indexed as a combination of Cr_3PtN and Cr_2N, with trace amounts of Cr_2O_3 as a minor phase (likely an impurity inclusion left over from the arc casting). The Cr_3PtN phase has been reported[20] to have a cubic *Pm*3*m* perovskite structure with a lattice parameter of $a = 3.879$ Å. A quantitative Rietveld analysis[21] refined to the following lattice parameters: $a = 3.8797$ Å for Cr_3PtN; $a = 4.8066$ Å and $c = 4.4817$ Å for Cr_2N; and $a = 4.948$ Å and $c = 13.58$ Å for Cr_2O_3. The phase fractions were determined to be Cr_3PtN (32.9 wt%), Cr_2N (64.5 wt%), and Cr_2O_3 (2.6 wt%). The identification by XRD of Cr_3PtN and Cr_2N is consistent with the SEM and EPMA data shown in Fig. 2.

TEM was used to further investigate and confirm that the Cr_3Pt phase nitrided to form the Cr_3PtN perovskite phase. Analysis was performed on arc-cast Cr-5Pt nitrided at 1100 °C for 48 h in the region where both the Cr(Pt) matrix phase and the Cr_3Pt dispersion were nitrided. Dispersed grains observed in the matrix of the nitrided precipitate phase were consistently identified

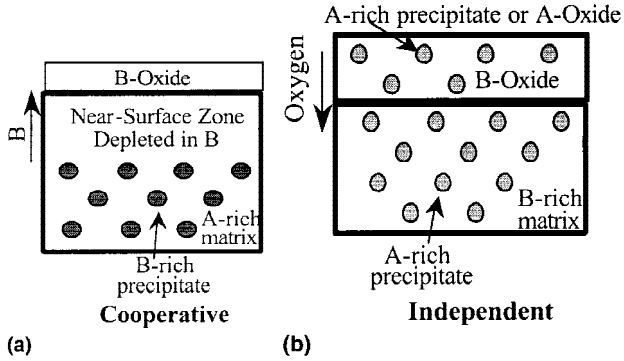

FIG. 1. Schematic limiting cases for reaction of a two-phase alloy (shown here for oxygen) (after Ref. 17).

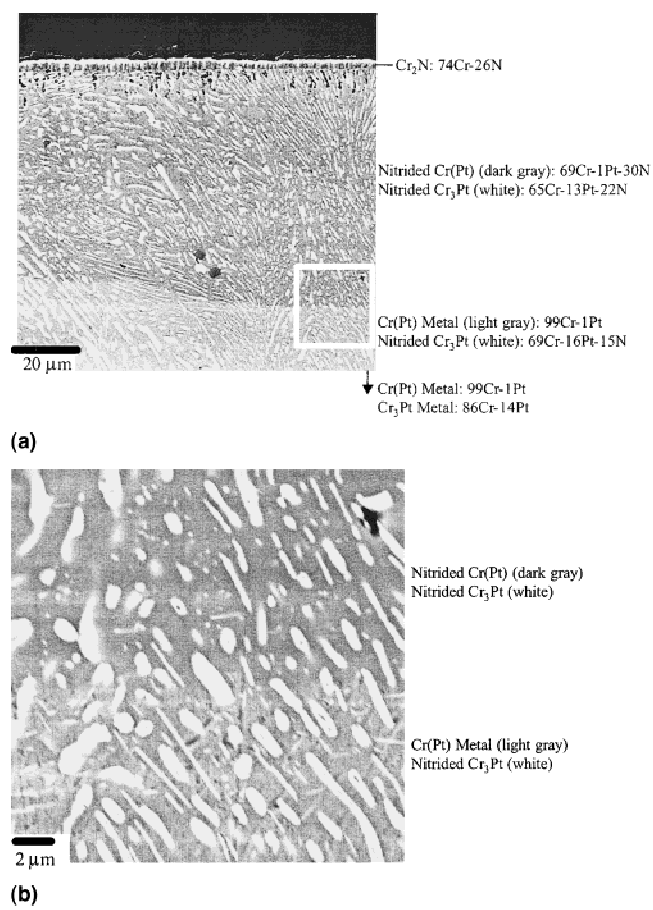

FIG. 2. SEM (secondary mode) cross-section micrographs of Cr-5Pt at.% heat treated at 1350 °C for 8 h, 1050 °C for 12 h, and then held in high-purity nitrogen at 1000 °C for 24 h: (a) low-magnification overview, (b) high-magnification view of boxed region in (a).

by x-ray energy dispersive spectroscopy (XEDS) to contain Cr and Pt [Fig. 4(a)]. The presence of nitrogen is not readily apparent in this spectrum due to absorption of characteristic low-energy x-rays. Qualitatively, different levels of strain were present in this phase since the spatial position of diffraction spots in selected-area diffraction (SAD) patterns obtained from large areas were systematically shifted relative to the center of disks in convergent-beam electron diffraction (CBED) patterns obtained from localized areas. Inhomogeneities in the magnitude of strain resulted in a range of calculated lattice *d* spacings from the SAD patterns that prevented an unambiguous determination of the crystal structure based on either the Cr_3Pt or Cr_3PtN phases (JCPDS files). However, symmetry may be used to differentiate between these two phases. The space group of Cr_3Pt is *Pm*3*n* whereas that of Cr_3PtN is *Pm*3*m*. These space groups belong to the same point group of *m*3*m*, which is consistent with the 3*m* symmetry observed in the CBED whole pattern of the ⟨111⟩ zone axis shown in Fig. 4(b). The *n*-glide plane symmetry contained in the Cr_3Pt structure indicates that a Gjonnes-Moodie (G-M) line should be present in kinematically forbidden 111 reflections[22] and this extra symmetry element can be used to differentiate between the two phases. Figure 4(c) shows the CBED whole pattern of the ⟨112⟩ zone axis; the observed 2*mm* symmetry does not show any evidence of the G-M line in the 111 reflection. Thus, the combined results of calculated lattice *d* spacings, interplanar angle, and symmetry are consistent with the Cr_3PtN perovskite phase based on the *Pm*3*m* space group, as indicated by the EPMA and XRD analysis. No evidence of the Cr_3Pt phase locally internally nitriding to form Cr_2N and Pt, rather than Cr_3PtN, was observed.

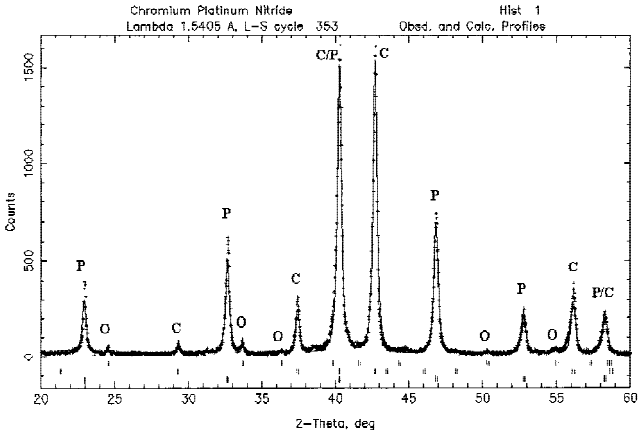

FIG. 3. XRD data for 1100 °C, 48-h nitrided cast Cr-5Pt at.% with detail from the Rietveld refinement showing the experimental data (points) overlaid with the calculated pattern (line). Below the patterns are indicated the peak positions for the three phases Cr_3PtN (P), Cr_2N (C), and Cr_2O_3 inclusions (O).

The microstructural characterization of the nitrided structure in Cr-5Pt is therefore consistent with nitridation of the Cr_3Pt precipitate phase to form single-phase (or nearly single-phase) Cr_3PtN perovskite. This result provides proof of principle that in-place internal oxidation in a two-phase alloy can be used to controllably synthesize a complex ceramic compound. The microstructural evidence suggests that the Cr_3PtN phase formed directly from Cr_3Pt, rather than a multistep process by solid-state reaction of intermediate formed phases such as Cr_2N and Pt. To our knowledge, this would be the first example of such a reaction path.

The potential utility of in-place internal oxidation as a synthesis approach comes from the high degree of control achievable by exploitation of the solid-state alloy phase equilibria and crystallographic relationships offered by the initial metallic alloy composition, e.g., the opportunity to "set" the template prior to the oxidation reaction. A staged process is envisioned beginning with the deposition of a metallic thin-film alloy (or possibly the surface region of a bulk alloy or single crystal) of carefully selected composition. Thermal treatment is used to precipitate the metallic dispersion, which patterns according to the crystallographic relationships with the

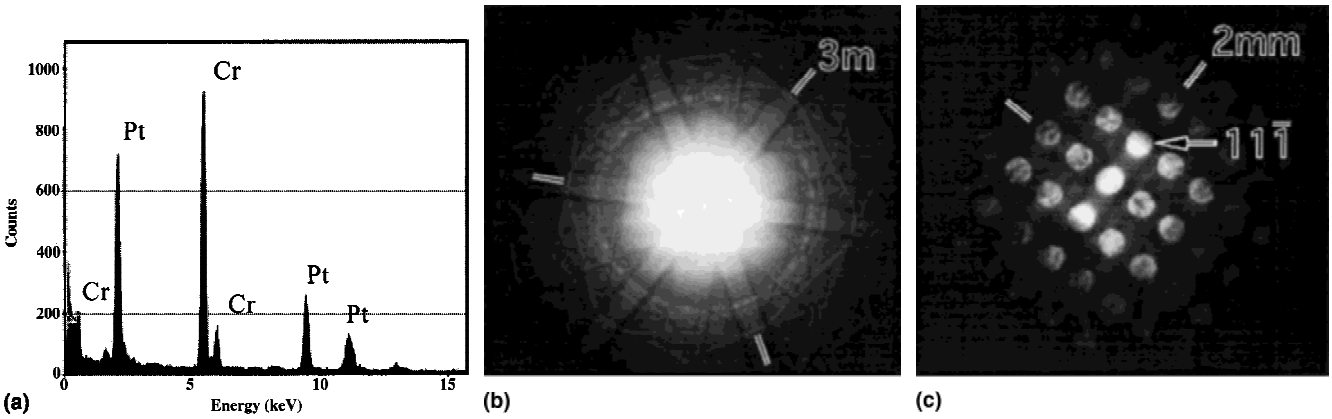

FIG. 4. TEM analysis of the dispersed phase in 1100 °C, 48-h nitrided cast Cr–5Pt at.% showing (a) XEDS spectrum of the composition and (b,c) CBED whole patterns of [111] and [112] zone axes consistent with 3*m* and 2*mm* symmetry, respectively, of the Cr_3PtN perovskite phase.

parent matrix. Once the initial two-phase alloy template is set, one or more reactive gaseous species are introduced under conditions that promote in-place internal oxidation. Depending on the kinetics associated with the reaction conditions, the activity (partial pressure) of the oxidant, and the nature of the metallic component(s), the matrix could remain metallic or be converted to crystalline or amorphous ceramic.

In some cases, it may be possible to produce the metallic precursor precipitates on a nano- or mesoscale to yield a corresponding nano-/mesoscale complex ceramic-phase dispersion. The energetics and structural relationships in the system and particulars of the precipitation/reaction conditions determine whether such a size scale can be achieved. The synthesis of nano-/mesoscale complex ceramic dispersions from an initially nano- or mesoscale metallic structure will likely only be possible for thin films ($\leqslant$1–10 microns thick), where the reaction can be accomplished rapidly and/or at relatively low temperatures to minimize the opportunity for coarsening.

Quantitative theoretical treatments are available for internal oxidation in single-phase alloys where the oxidant atoms have a much higher mobility than the solute atoms[23,24] and for many cases of binary, two-phase alloy oxidation (reviewed in Ref. 17). From a simple, qualitative viewpoint, in-place internal oxidation is kinetically favored for metallic matrix phases that exhibit a high permeability to a given oxidant (e.g., nitrogen, but not oxygen, in chromium or oxygen, nitrogen, and carbon in titanium). The key prerequisite in selecting systems potentially amenable to this approach is that a suitable precipitation reaction must exist and yield a precursor metallic precipitate phase with a similar metal component stoichiometry to the desired complex ceramic phase. Precursor alloy structures based on transition or refractory metal matrices with high permeability to interstitial compound forming reactants such as nitrogen or carbon appear to be especially fruitful ground. Some potential binary precursor candidate systems (containing precipitation reactins capable of yielding a compound phase in a dilute solid solution matrix) are listed in Table I.

TABLE I. Partial compilation of some potential binary precursor systems (ternary and higher order precursor systems are also amenable to this approach).

Matrix	Potential precursor phase
Cr	Cr_3Ge, Cr_3Pt, Cr_3Rh, Cr_2Ti
Cu	Cu_2In, Cu_4Ti
Fe	Fe_2Mo, Fe_2Nb, $Fe_{1-x}Se$, Fe_2Ta, Fe_2Ti
Mn	Mn_2Hf, Mn_2Sb, Mn_2Ti
Mo	Mo_2Co, $MoPd_2$, MoPt, MoRh, MoRu, Mo_3Si, Mo_2Zr
Ni	$Ni_{17}Gd_2$, Ni_3In, Ni_3Nb, Ni_3Sn, Ni_8Ta
Nb	NbFe, Nb_6Ge, Nb_3Sb, Nb_5Si_3, $NbSn_2$
Ru	RuTi
Ta	TaFe, Ta_2Ni, TaPd
Ti	Ti_3Bi, Ti_2Co, Ti_2Cu, TiFe, Ti_5Ge_3, TiMn, Ti_4Sb
V	V_3Ge, V_2Hf, V_3Ni, V_2Zr
Zr	Zr_2Bi, Zr_4Fe, Zr_3In, $ZrMn_2$, ZrRu, ZrV_2, ZrW_2, Zr_2Zn

ACKNOWLEDGMENTS

M.P.B.'s interest in using oxidation reactions to synthesize structures, (especially at the nanoscale) was initiated by J. Doychak of NASA Glenn, based on Doychak's observations of nanoscale structures during pesting of $NbAl_3$ and $MoSi_2$ intermetallics. The authors thank B. Gleeson, F. Gesmundo, H. Christen, and D.L. Lowndes for many helpful discussions, M.K. Miller and R.A. McKee for reviewing this manuscript, and J.W. Jones for preparing TEM specimens of nitrided alloys for analysis. This research was sponsored by the Oak Ridge National Laboratory LDRD SEED program and the Fossil Energy Advanced Research Materials Program. S.K. Wrobel was funded by NSF through an IGERT Program (DGE-9987548).

REFERENCES

1. C.S. Smith, Min. Met. **11,** 213 (1930).
2. F.N. Rhines, Trans. Am. Inst. Min. (Metall.) Eng. **137,** 246 (1940).
3. J.L. Meijering, in *Advances in Materials Research*, edited by H. Hermann (Wiley, New York, 1971), Vol. 5, pp. 1–81.
4. P.P. Swan, S. Weissmann, and D.F. Wriedt, Trans. Amer. Inst. Min. (Metall.) Eng. **230,** 1306 (1964).
5. R.A. Rapp, Corrosion **21,** 382 (1965).
6. J. Nagamatsu, N. Nakagawa, T. Muranaka, Y. Zenitani, and J. Akimitsu, Nature **410,** 63 (2001).
7. K.D. Kreuer, Chem Mater. **8,** 610 (1996).
8. A.P. Ramirez, J. Phys. Condens. Matter **9,** 8171 (1997).
9. J.M.D. Coey, M. Viret, and S. von Molnar, Adv Phys. **48,** 167 (1999).
10. R. Niewa and F.J. DiSalvo, Chem. Mater. **10,** 2733 (1998).
11. D.H. Gregory, J. Chem. Soc., Dalton Trans. 259 (1999).
12. J. Megusar and G.H. Meier, Metall. Trans. A **7,** 1133 (1976).
13. J. Stringer, P.S. Corkish, D.P. Whittle, in *Stress Effects and Oxidation of Metals*, edited by J.V. Cathcart (Met. Soc. AIME, New York, 1975), p. 75.
14. B.D. Bastow, G.C. Wood, D.P. Whittle, Oxid. Met. **16,** 1 (1981).
15. G. Wahl, Thin Solid Films **107,** 417 (1983).
16. G. Wang, B. Gleeson, and D.L. Douglass, Oxid. Met. **35,** 333 (1991).
17. F. Gesmundo and B. Gleeson, Oxid. Met. **44,** 211 (1995).
18. H. Spengler, Metall. **13,** 646 (1959).
19. F. Gesmundo, Y. Niu, and F. Viani, Oxid. Met. **43,** 379 (1995).
20. M. Nardin, G. Lorthioir, M. Barberon, R. Madar, E. Fruchart, and R. Fruchart, C.R. Acad. Sci. Paris **274,** 2168 (1972).
21. A.C. Larson and R.B. von Dreele, *GSAS–General Structure Analysis System*, LAUR 86-748, Los Alamos, NM (GSAS For Macintosh copyright A.C. Larson, 2001).
22. B.F. Buxton, J.A. Eades, J.W. Steeds, and G.M. Rackham, Philos. Trans. R. Soc. **281,** 181 (1976).
23. G.R. Laflamme and J.E. Morral, Acta Metall. **26,** 1791 (1978).
24. E.K. Ohriner and J.E. Morral, Scripta Met. **13,** 7 (1979).